Electronic Supplementary Material (ESI) for Journal of Materials Chemistry C.
This journal is © The Royal Society of Chemistry 2020

J. Mater. Chem. C

Coexistence of Relaxor Behavior and Ferromagnetic Order in Multiferroic $Pb(Fe_{0.5}Nb_{0.5})O_3$-$BiFeO_3$ Solid Solution

Haijuan Li[1], Jian Zhuang[1,*], Alexei A. Bokov[2], Nan Zhang[1], Jie Zhang[1],Wei Ren[1,*], and Zuo-Guang Ye[2,*]

[1] Electronic Materials Research Laboratory, Key Laboratory of the Ministry of Education & International Center for Dielectric Research, Xi'an Jiaotong University, Xi'an 710049, China

[2] Department of Chemistry and 4D LABS, Simon Fraser University, Burnaby, British Columbia, V5A 1S6, Canada

* Corresponding Authors: zye@sfu.ca (Z.-G. Ye); jzhuang@xjtu.edu.cn (J. Zhuang); ; wren@xjtu.edu.cn (W. Ren)

Supplementary Materials

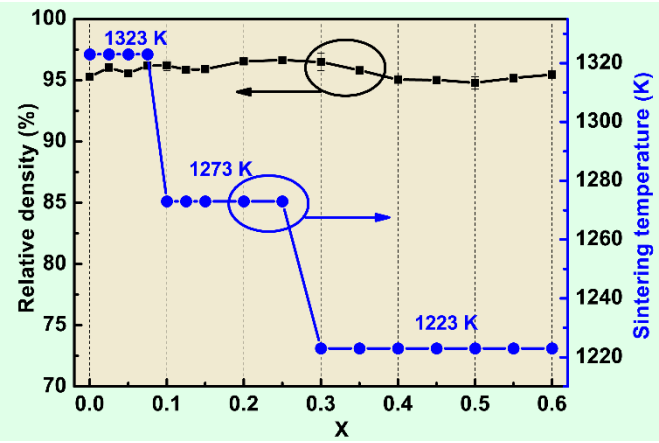

Figure S1. Variation of the relative density (ρ) of the ceramics of the (1-*x*)PFN-*x*BFO solid solution sintered at different temperatures depending on composition.

Table S1. Detailed information on the XRD Rietveld refinement results of the PFN-BFO solid solution for the compositions with $x \leq 0.4$

x	*Cm*					$Pm\bar{3}m$		*r*-factor		
	a (Å)	b (Å)	c (Å)	β (°)	phase (%)	a (Å)	phase (%)	r_{wp}	r_{exp}	r_p
0	5.6732(3)	5.6722(4)	4.01586(8)	90.034(3)	100			11.7	11.2	8.4
0.025	5.6708(2)	5.6696(1)	4.01604(6)	89.942(2)	54.9(2)	4.01186(3)	45.1(1)	10.9	10.6	7.7
0.05	5.6708(2)	5.6697(2)	4.01537(6)	90.056(2)	57.3(1)	4.01162(3)	42.7(1)	11.3	10.9	7.9
0.075	5.6702(2)	5.6690(2)	4.01481(7)	90.054(2)	57.2(3)	4.01109(3)	42.8(1)	11.1	10.8	7.8
0.1	5.6707(4)	5.6693(5)	4.0173(1)	90.057(5)	41.2(2)	4.01106(5)	58.8(4)	11.2	7.7	7.1
0.125	5.6700(9)	5.6694(9)	4.0153(1)	90.039(6)	45.9(1)	4.01026(9)	54.1(2)	11.1	7.6	6.9
0.15	5.6684(6)	5.6674(6)	4.0144(1)	90.047(5)	39.8(3)	4.00969(5)	60.2(4)	11.1	7.2	6.9
0.2	5.6671(4)	5.6659(4)	4.0147(2)	90.077(4)	36.7(1)	4.00891(4)	63.3(4)	10.4	8.2	6.6
0.25	5.6652(9)	5.6636(9)	4.0164(3)	90.070(9)	32.2(2)	4.00854(7)	67.8(2)	11.6	9.0	7.8
0.3	5.6642(7)	5.6283(4)	4.0394(3)	89.626(8)	8.2(3)	4.00577(2)	91.8(2)	7.9	6.4	6.1
0.35						4.00441(3)	100	10.0	6.5	7.7
0.4						4.00277(3)	100	9.1	6.4	6.9

Table S2. The Bragg peak positions in terms of 2theta angle from XRD Rietveld refinement results using the *Cm* and $Pm\bar{3}m$ phases, respectively, and the FWHM values of the (110) and (111) peaks for (1-*x*)PFN-*x*BFO solid solution (x = 0, 0.1, 0.2, 0.3, and 0.4).

Composition x	Peak position (°)				FWHM	
	Cm		$Pm\bar{3}m$		Test data	
	(110)	(111)	(110)	(111)	(110)	(111)
0	31.54	38.85			0.0721	0.0617
0.1	31.53	38.90	31.56	38.87	0.0719	0.0618
0.2	31.57	38.90	31.54	38.88	0.0720	0.0618
0.3	31.55	38.88	31.55	38.86	0.0698	0.0603
0.4			31.56	38.86	0.0691	0.0590

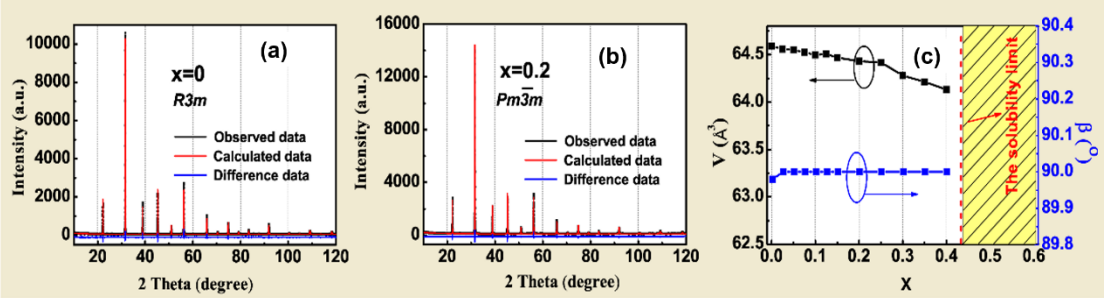

Figure S2. Rietveld refinements results using the *R3m* and $Pm\bar{3}m$ symmetries for (a) $x = 0$ and (b) $x = 0.2$, respectively. (c) Variations of the unit cell volume and angle β of the (1-x)PFN-xBFO solid solution with composition.

Table S3. Detailed information on the XRD Rietveld refinement results of the PFN-BFO solid solution using the *R3m* and $Pm\bar{3}m$ phases for the compositions with $x \leq 0.4$.

x	Space group	a (Å)	r_{wp}	r_{exp}	r_p	β (°)
0	*R3m*	4.01225(3)	12.2	11.2	8.8	89.996(2)
0.025		4.01159(2)	11.5	10.6	8.3	90
0.005		4.01143(2)	12.1	10.9	8.8	90
0.075		4.01092(3)	11.9	10.8	8.7	90
0.1		4.01032(5)	12.5	7.7	8.3	90
0.125	$Pm\bar{3}m$	4.01052(3)	11.3	7.6	7.2	90
0.15		4.00971(2)	11.3	7.2	7.2	90
0.2		4.00900(3)	10.7	8.2	6.9	90
0.25		4.00867(5)	11.8	9.0	8.1	90
0.3		4.00582(2)	8.6	6.4	6.5	90
0.35		4.00441(3)	10.0	6.5	7.7	90
0.4		4.00277(3)	9.1	6.4	6.9	90

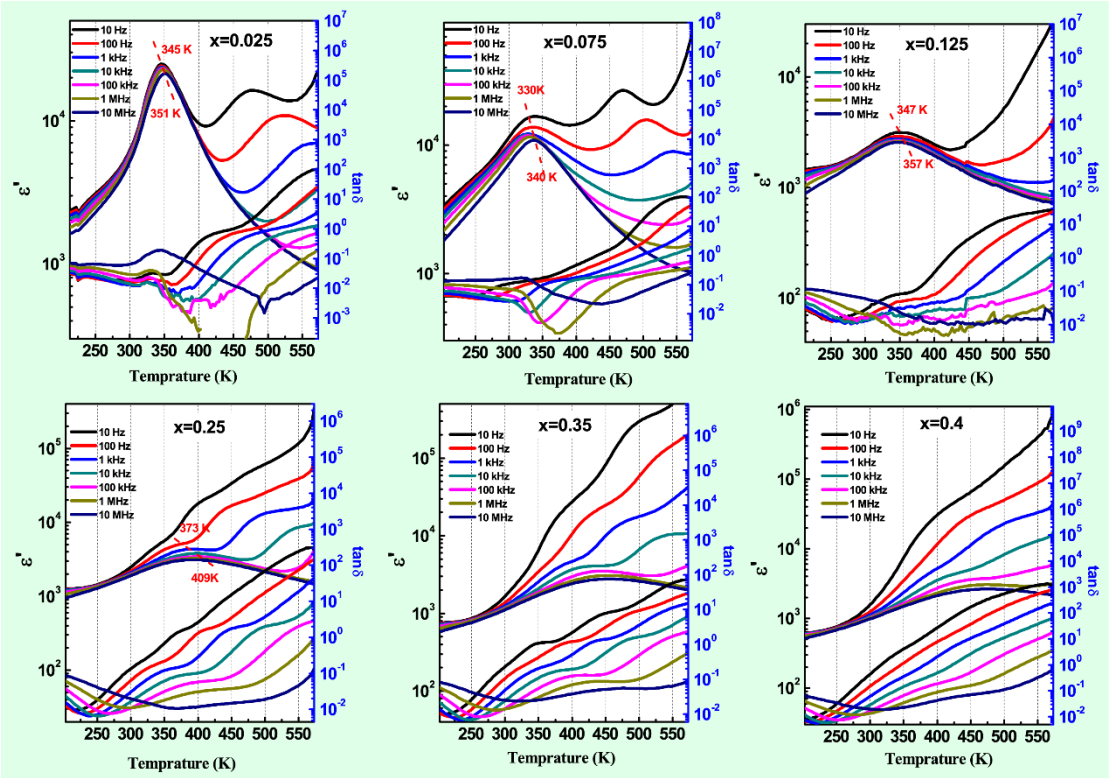

Figure S3. Temperature dependences of the dielectric permittivity (ε') and loss tangent ($tan\delta$) for the (1-x)PFN-xBFO (x = 0.025, 0.075, 0.125, 0.25, 0.35, and 0.4) ceramics measured at different frequencies.

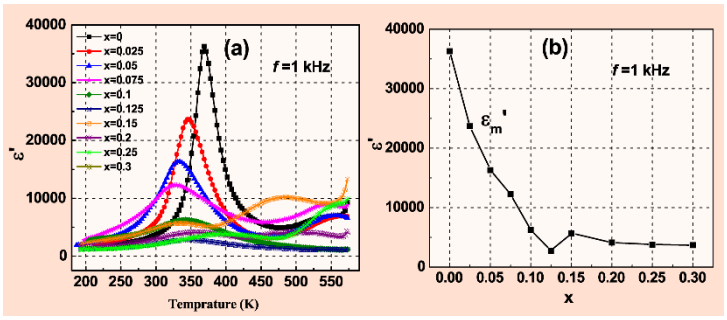

Figure S4. (a) Temperature dependences of the dielectric permittivity (ε') for (1-x)PFN-xBFO (x = 0, 0.025, 0.05, 0.075, 0.1, 0.125, 0.15, 0.2, 0.25 and 0.3) ceramics measured at 1 kHz. (b) Variation of ε_m' at 1 kHz as a function of composition for the (1-x)PFN-xBFO ceramics.

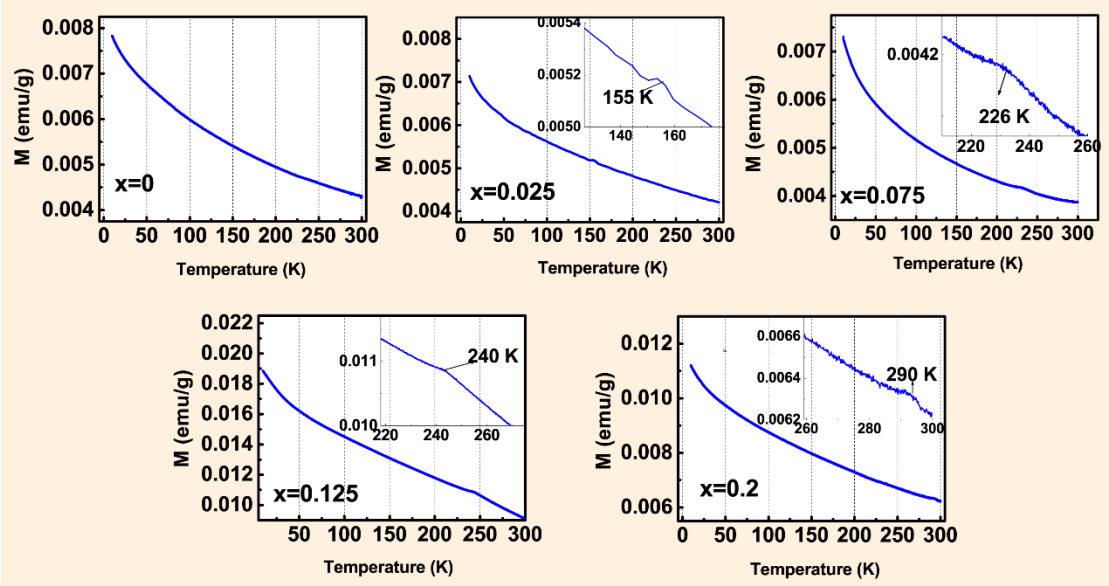

Figure S5. The M(T) curves of the (1-*x*)PFN-*x*BFO ceramics (*x* = 0, 0.025, 0.075, 0.125 and 0.2) measured upon heating from 5 K to 300 K under a field of 500 Oe after field cooling. The insets are the enlarged views.

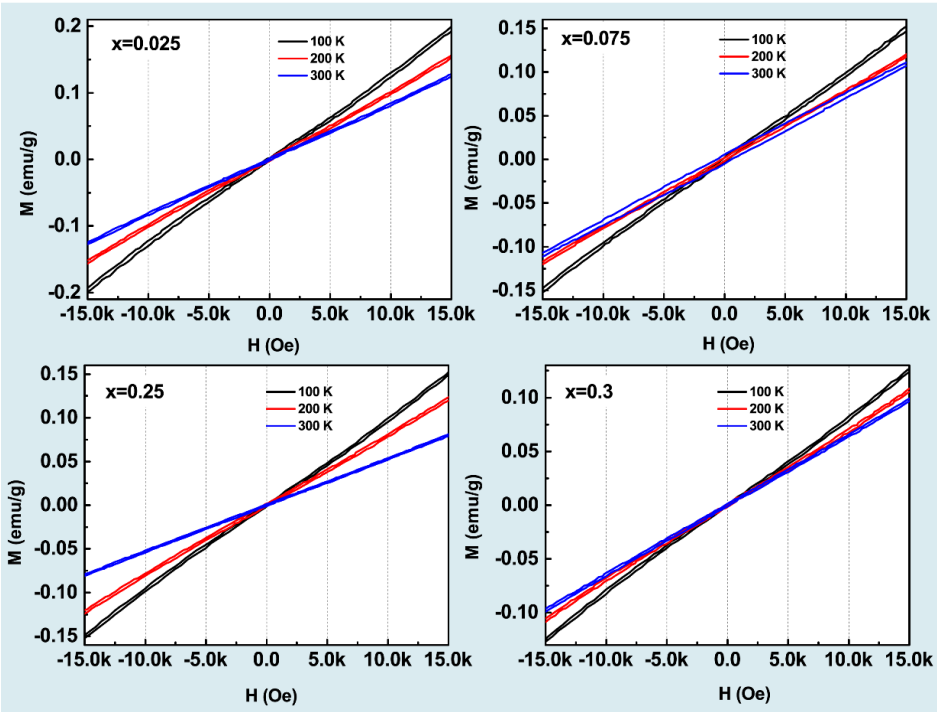

Figure S6. The magnetic hysteresis loops of the (1-*x*)PFN-*x*BFO ceramics (*x* = 0.025, 0.075, 0.25 and 0.3) measured at 100 K, 200 K and 300 K.